Available online at www.sciencedirect.com

ScienceDirect

Energy Procedia 86 (2016) 479 – 488

Energy Procedia

The 8th Trondheim Conference on CO_2 Capture, Transport and Storage

Medium scale CO2 releases

J. Hébrard [a]*, D. Jamois [a], C. Proust[a,c], M. Spruijt[b], C.E.C. Hulsbosch-Dam[b], M. Molag[b] and E. Messina[b]

[a]*INERIS, dept PHDS, Parc Technologique ALATA BP 2, 60550 Verneuil-en-Halatte, France*
[b]*TNO, Dept. Urban Environment and Safety, Princetonlaan 6, 3585 CB, UTRECHT, Netherlands*
[c]*Sorbonne Universities, UTC, ESCOM, EA 4297 TIMR laboratory, centre Pierre Guillaumat, 60200 Compiègne, France*

Abstract

The scale of proposed carbon dioxide (CO_2) capture and storage (CCS) chains also draws attention to the hazards posed by the transport mode, enabling the link from source to sink. As such, the adverse consequences of an accidental release from transport pipelines or other equipment containing CO_2 at high pressure in a dense-phase (supercritical or liquid) state are (re)considered in theory and in practice. Several experimental observations of large-scale CO_2 releases have been made, and yet the physics and thermodynamics involved are not fully understood. The work presented here provides a database focused on the specificities of the release and the dispersion of the carbon dioxide cloud in case of substantial variations of storage (temperature and pressure) and discharge conditions (nozzle size).

Peer-review under responsibility of the Programme Chair of the 8th Trondheim Conference on CO_2 Capture, Transport and Storage

Keywords: CO_2, supercritical, accidental release, transport pipeline, full bore release

* Corresponding author. Tel.: +33-3 44 55 69 19; fax: +33- 3-44-55-62-00.
E-mail address: Jerome.hebrard@ineris.fr

Peer-review under responsibility of the Programme Chair of the 8th Trondheim Conference on CO_2 Capture, Transport and Storage
doi:10.1016/j.egypro.2016.01.049

1. Introduction

Aiming at reducing the global warming (the "greenhouse effect"), the injection of carbon dioxide (CO_2) underground in geological formations is commonly identified as a necessary mid-term solution, envisioning an ideal zero emission (post hydrocarbon energy) era ahead. This alternative plan to today's common practice – the atmospheric release of carbon dioxide - is known as Carbon Capture and Storage (CCS). Following this route, CO_2 would be captured from the exhaust of fossil fuel fed power plants, transported to a storage site, and finally injected into the sub-surface [1]. A particularly sensitive part of the CCS chain, from a safety point of view, is the transport of large amounts of CO_2. Depending on the distances from CO_2 'source to sink' and quantities involved per case (see for example [2]) either vessels or pipelines will be used for transport. While transported, a loss of containment may occur, where a large amount of CO_2 could be accidentally released in the atmosphere – possibly in an urban environment, carrying not only the toxicity of CO_2, but potentially also of the noxious impurities contained. The acceptability of CCS technologies depends partly on such safety issues. The present work is a contribution to this point.

The most economically feasible way of transporting CO_2 by pipeline is with CO_2 in a dense state, i.e. compressed liquid or supercritical conditions. The supercritical condition (temperature above 304 K, and pressure above 73.8 bar) has the advantage of a reduced viscosity and increased density. However, the supercritical state means corrosion issues [3].

In recent years, several projects have considered the hazards linked with heavy cloud dispersion and focused on the development of experimental databases. For example, large scale experiments were focused on cloud dispersion from massive releases [4] or [5]. In addition, some models were developed or 'upgraded' for CO_2 [6], [7] and [8]. Some projects focused on the presence of impurities and their influence on the thermodynamical properties of the mixture or their toxic behaviour [9].

Among the different experimental campaigns focused on the safety of the CCS chain, only a few were dedicated to the influence of the initial conditions on the safety distances. In the current paper, INERIS and TNO, using an original experimental set-up developed within European projects [10], focus on:

1- The thermodynamical behaviour of the flow during a rapid blowdown of a vessel, i.e. to have a better understanding of CO_2 two-phase flow in a short pipe and improve the calculation of the source term. The full bore rupture is a frequently studied safety-related scenario.
2- The influence of the conditions (supercritical vs saturated) and how supercritical initial storage conditions will affect the effect distances in CO2 release scenarii.

2. Presentation of the test rig

The experimental releases were from a 5 m pipe connected to 2 m3 vessel. The vessel is equipped with three flanges (two on the side, and one on the top, see Figure 1). One flange is equipped with a 2" internal diameter hole, which is prolonged internally with a 2" internal diameter and 5.6 m long bended pipe plunging at the bottom of the sphere. In this configuration, the liquid CO2 at the bottom of the vessel is then preferentially pushed into the pipe as long as the level of the liquid phase is higher than 5 cm.

The internal pressures in the sphere and in the pipe are monitored using four pressure transducers: piezoresistive KISTLER type 4045 A 200; 0 – 200 bar ± 0,2 bar. Five thermocouples are also displayed in the sphere (T1 & T2) and in the pipe (T3, T4 and T5) (Figure 1). They are K type in a steel sleeve, 1 mm, class A.

Immediately outside the vessel (Figure 1) two successive isolation valves (one manual and one remotely actuated) are installed on the 2" inner diameter pipe. Very close to the release end, a third isolation valve (remotely actuated) is mounted, just upstream of the orifice holder.

The vessel is laid on 4 electronic weighing load cells (METTLER TOLEDO 250-2000 kg ±1 kg) to measure the

evolution of the content of CO2 during filling operations and release. With a measured total decrease of mass of 50 kg, the error on the mean mass flow rate is not greater than ±5%. By derivation of the experimental curve giving the mass as function of time, the instantaneous mass flow rate can be obtained. The experimental error is about ±10% if the raw signal is averaged over 20 data points (representing 2 s for a data acquisition rate of 10 Hz).
For certain experiments, an orifice holder was mounted (with 3.5 or 5 mm hole diameter) at the very end of the pipe. But experiments were also performed without the nozzle, i.e. with an outflow diameter of 50 mm. The initial pressure and temperature inside the vessel correspond either to saturated conditions or supercritical conditions.

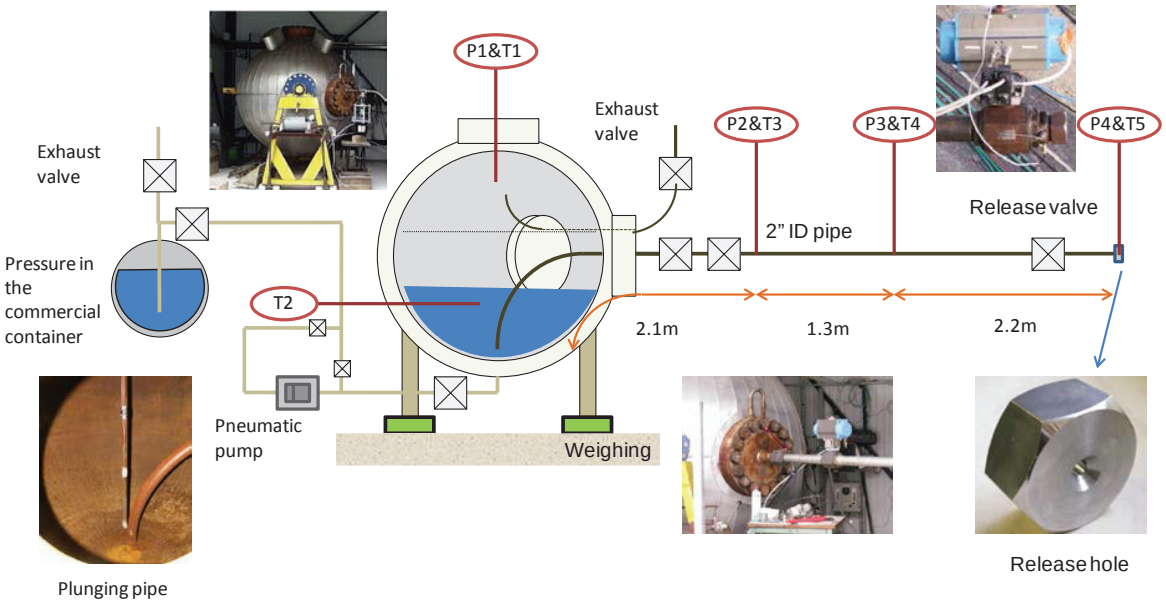

Figure 1: Experimental equipment

Figure 2: Pictures of the cloud extracted from videos (full bore rupture) taken from different viewing angles.

During each release, pressure and temperature were measured inside the vessel and the pipe, and temperature and concentration were measured in the cloud. Video images were used to capture the appearance of the jet. The details of the experiments can be found in [10].

3. Experimental procedure

To fill the sphere, commercial containers (300 kg CO_2 each at about 50 bar) are connected directly to the bottom valve (Figure 1). As soon as liquid CO_2 enters the sphere (P1>P2), it vapourizes and the internal temperature strongly decreases. As a result a differential pressure between P1 and P2 is maintained and drives the liquid flow rate as long as the temperature in the bottom part of the sphere stays below the temperature in the container. At the equilibrium point (between the sphere and the container) about 300 kg of CO_2 were transferred. The rest of the liquid was then pumped (actually the longer step).At ambient conditions (25°C), CO_2 is mostly liquid in the sphere with a vapour pressure of about 60 bar.

The following protocol is followed:

- Filling of the pipe by purging via a short opening on the end-of-pipe release valve, just before the release, the pipe is then filled with liquid CO_2
- Control of the instrumentation (mass, sensors, camera),
- Release until the targeted mass loss,
- Emptying the pipe.

The initial conditions of the trials are presented on the next table:

Table 1: Initial conditions

Pressure	Temperature (liquid)	Temperature (ambiant)	Humidity	Orifice diameter	Configuration
[bar]	[°C]	[°C]	[%]	[mm]	[-]
59.6	~22	19	71	2	Saturation
60.3	~22	21.6	54	2	Saturation
59.4	~22	15	76	2	Saturation
59	22.3	13.1	85	3.5 mm	Saturation
59.1	~22	18	66	5 mm	Saturation
58.7	21.9	14.8	81	5 mm	Saturation
91.1	41.3	14.9	81	3.5 mm	Super-critical
89.3	40.7	15.6	79	5 mm	Super-critical
60.4	23.2	13.9	92.9	5 mm	Saturation (long)
62.2	24.5	20.3	75.3	50 mm	Emptying

4. Results and discussion

4.1. Full bore rupture: Phases in the release

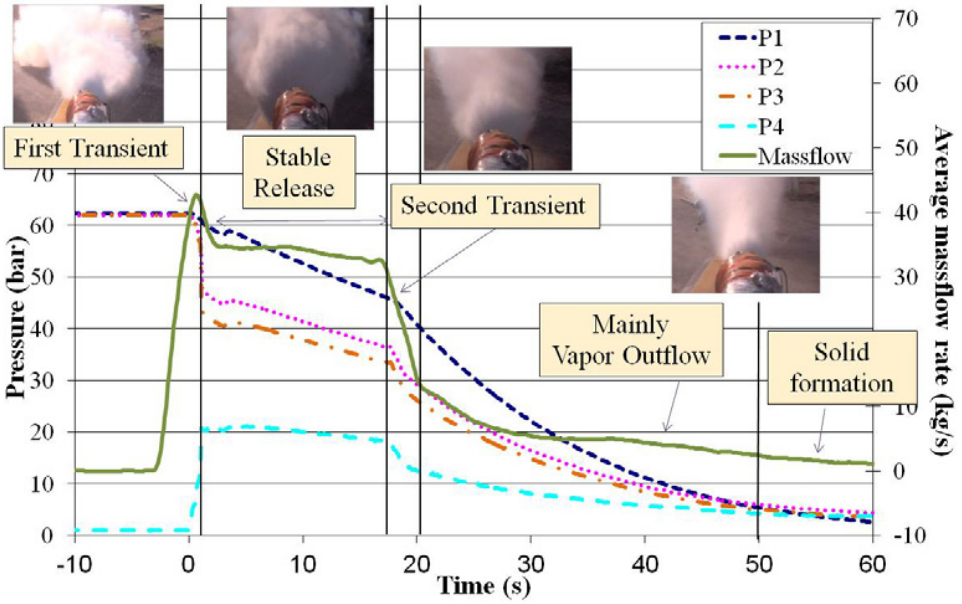

Figure 3: Average mass flow rate and pressure at various locations during full bore release. Photographs show the typical appearance of the jet at each stage.

The mass flow rate as a function of time is plotted in Figure 3. Based on photos of the jet, on the P,T curves, on the position of the liquid level inside the sphere (more detailed are given in the following sections), the Full Bore Release (FBR) can be divided into 5 different stages. The first transient is an initial phase of the release. After this initial phase a stable release is reached, were the mass flow rate is constant for about 17 seconds. During this period the pressure inside the vessel and the pipe decreases somewhat, however, the 'steady state' mass flow rate is not affected. After about 18 seconds there is a second transient. During this transition both the mass flow rates and the pressure undergo a significant drop. Also during this drop the shape of the cone of CO_2 leaving the pipe becomes narrower, see Figure 3. After the transient the pressures continue to drop fast and the drop in mass flow rate decreases. After 50 seconds the pressure and temperature inside the vessel drop below the triple point. The whole process is summarized in Table 2.

Table 2: Summary of stages during full bore CO_2 release – hole size 50 mm.

Time	Name/description	Main processes
0 to 1 sec	1st transient	Build-up of liquid outflow
1 to 18 sec	Stable release	Liquid outflow
18 to 20 sec	2nd transient	Liquid level in vessel reaches the inlet of the pipe
20 to 50 sec	Decreasing outflow	Vapour outflow
After 50 sec	Final outflow	Vessel below triple point p&T

4.2. Full bore rupture: liquid level in the vessel

Figure 4 shows the calculated liquid surface position inside the vessel. The depth of the liquid pool is defined setting "zero" to the bottom of the sphere (no more liquid in the vessel). The main parameter used to obtain this parameter is the residual mass inside the vessel. But, at the very end of the release only solid and vapour CO_2 remain in the

vessel with a maximum estimated mass of 10 kg. However, at this moment a final weight of 79 kg is measured. It is believed that some drift of the measurement occurred probably due to some contraction of the metal parts. Following an offset of 69 kg was applied on the mass measurements to obtain Figure 4. The liquid level shows a steady decrease up to 20 seconds. At that moment the liquid level reaches the pipe inlet. Afterwards, mainly vapour could exit the vessel.

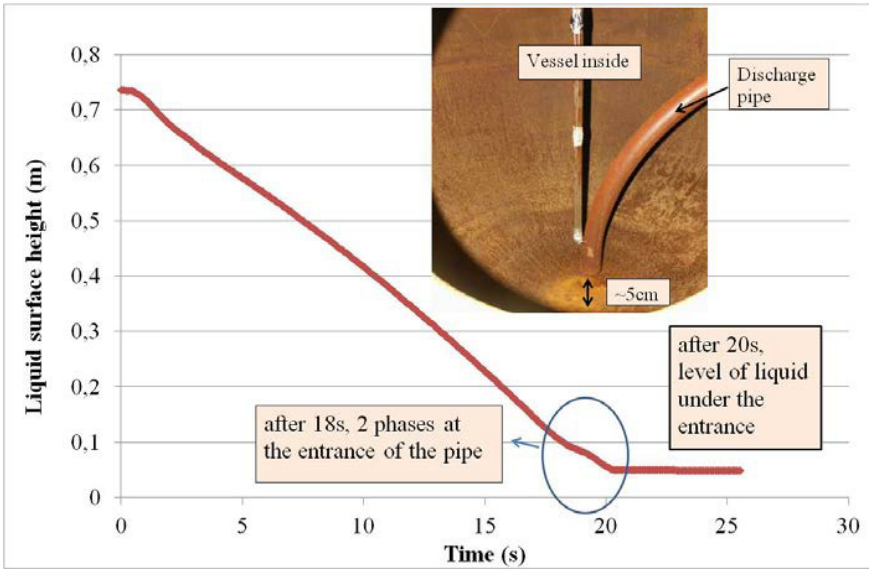

Figure 4: Liquid level inside the vessel versus time. After 20 seconds the liquid level drops below 5 cm, which is the height of the pipe entrance.

4.3. Full bore rupture: pT and pH diagrams

An important piece for the interpretation is the pressure and temperature evolutions at different locations, see Figure 5. For the largest part of the release, the measured p and T follow approximately the equilibrium line (VLE). Just before opening the valve the pressure and temperature in the vessel and 2 locations in the pipe are identical. Directly after opening the valve, the pressure in the pipe drops, quickly followed by a temperature drop, which restores the fluid at these positions to equilibrium. The pressure at the exit starts at only 22 bar, but the pressure remains roughly on the VLE curve. (Start-up effects at the exit are left out in this graph.) The temperatures along the pipe are very low (below -30 °C) and the pressure sensors drift so that the readings deviate from the actual values.

The results can also be displayed on a pressure-enthalpy (pH) diagram (Figure 6). The initial position in this diagram based on the void fraction calculation (Figure 7) depends on the amount of mass inside the vessel before opening the valve. As the scale is known to have some fluctuations over time the exact mass inside the vessel at a certain time is unknown. These long term fluctuations do not influence the mass flow rate measurements during releases, however, for measuring the amount of fluid still inside the vessel the off-set becomes important. If a 69 kg mass off-set is used, the resulting pH curve shown in Figure 6 reaches the dew point (green line). The various phases of the release are identified using different colours (blue for the liquid release, orange for the first transient,...). During the full liquid release, the reduction of the volume of liquid is compensated by CO2 evaporation, leading to a temperature and pressure drop according to the VLE. At time 18 s, the liquid level is close to the inlet of the pipe and since the liquid is probably boiling, a two-phase flow through the pipe is expected. After time 20 seconds, the liquid surface is below the inlet of the pipe and a mostly gaseous outflow is expected. Interestingly, the p-H curve follows for a while the dew point line suggesting some vaporising droplets are entrained. After this, the p-H trajectory enters again the two-phase part of the diagram and follows more or less a constant density line. It is believed that the expansion of the vapour causes some condensation which compensates more or less for the cooling of the vapour.

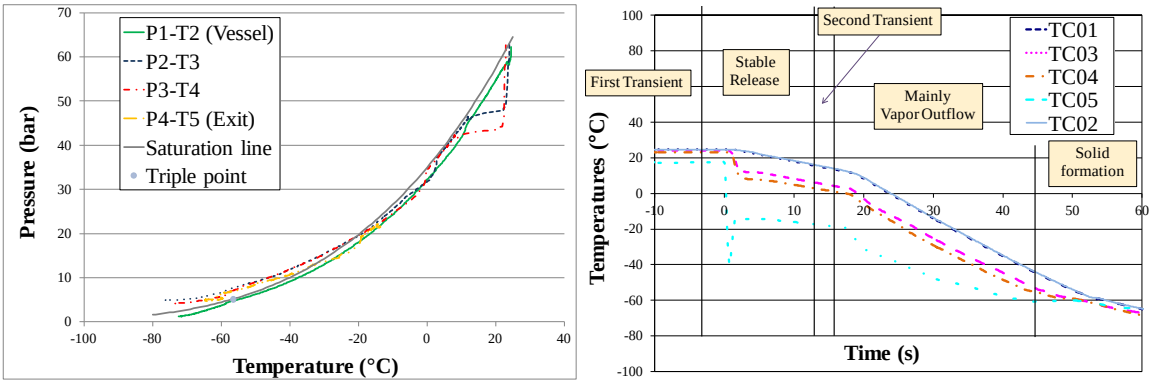

Figure 5 Left: PT-diagram for the vessel and 3 positions in the pipe. The black line indicates the saturation line. For temperatures above -56.6°C, this indicates equilibrium between liquid and vapour. Below this temperature, it is an equilibrium between solid and vapour.
Right: temperatures vs time

The p-H diagram at the exit location is obtained similarly (Figure 6). The different phases are also colored marked for both locations. In the first few seconds the flow is mostly liquid (blue) at the entrance of the pipe and the quality in the vessel is higher than the quality at the exit. The steel of the pipe heats the liquid inside the pipe, allowing the liquid to evaporate. After a few seconds, the pipe has cooled down. The quality at the exit of the pipe becomes greater than in the vessel. The flow is then sub-cooled by the expansion of the fluid in the pipe. Liquefaction within the pipe is then possible. When the flow becomes two phase at the entrance (orange), the quality at the exit becomes greater than in the vessel. After this moment, the flow remains sub-cooled in the pipe until the end of the release. The different photographs taken at the different stages (Figure 3) show the presence of a white core in the supersonic core of the jet. This seems to confirm the presence of liquid inside the jet, all along the release.

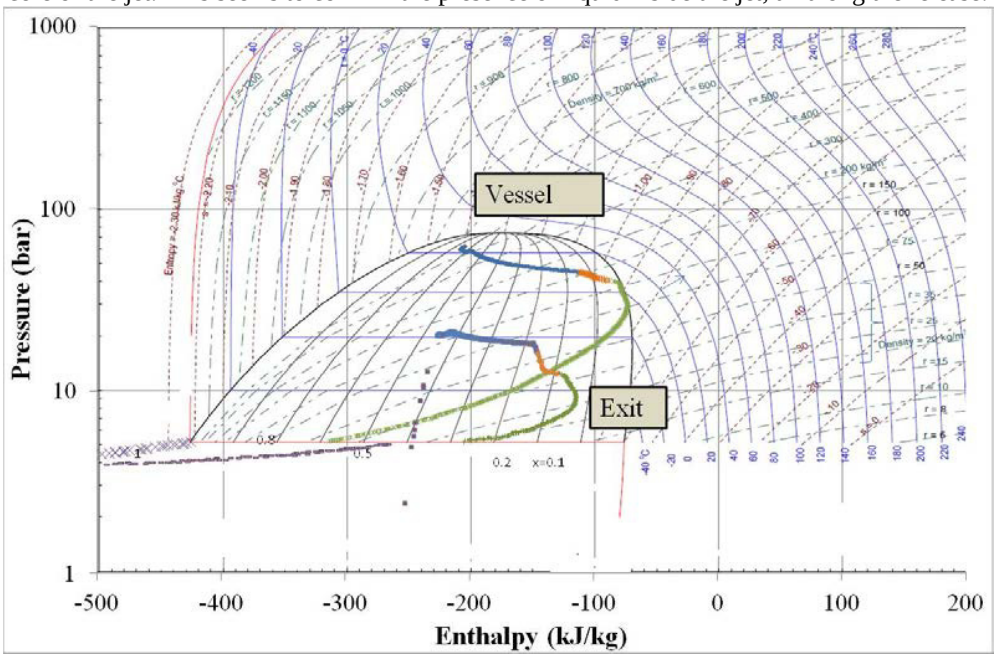

Figure 6 pH-diagram: vessel and exit, the different colours indicate the different stages; blue: first transient and stable liquid outflow, orange:2nd transient, green: mainly vapour outflow, purple: conditions inside the vessel below the triple point.

4.4. Full bore rupture: mass flow rates

From a safety point of view, the released mass is an important parameter. This is found from direct measurements and is discussed above. However, also the release velocity is important for the mixing and dispersion processes. This is parameter cannot be directly measured. It can be calculated if the density of the released fluid is known. This is dependent on the void fraction of the fluid released.

A simple way of looking at the fluid that exits the vessel is based on the average vessel void fraction. The principle is shown in Figure 7. At every moment the pressure, temperature and mass of CO_2 inside the vessel is known. Based on the assumption of a uniform pressure and temperature in the vessel, the density of the vapour and liquid can be determined from [11]. (Note that a uniform distribution of liquid and vapour is not a prerequisite.) This leads to an average void fraction in the vessel. This results in the liquid and vapour mass inside the vessel. When these quantities are known for every moment, also the mass flow rate of vapour and liquid can be calculated. The resulting curves for the full bore release are shown in Figure 8.

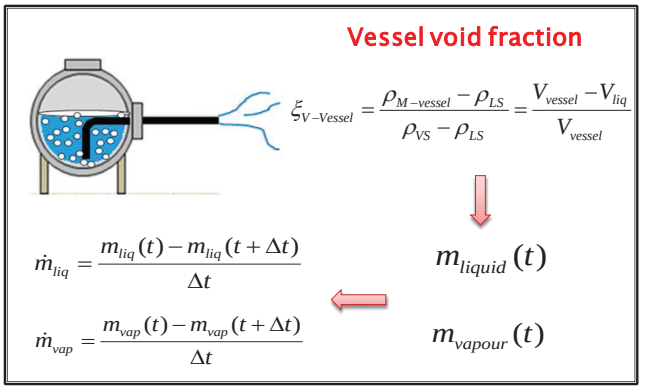

Figure 7 Calculating vapour and liquid mass flow rate out of the vessel into the pipe.

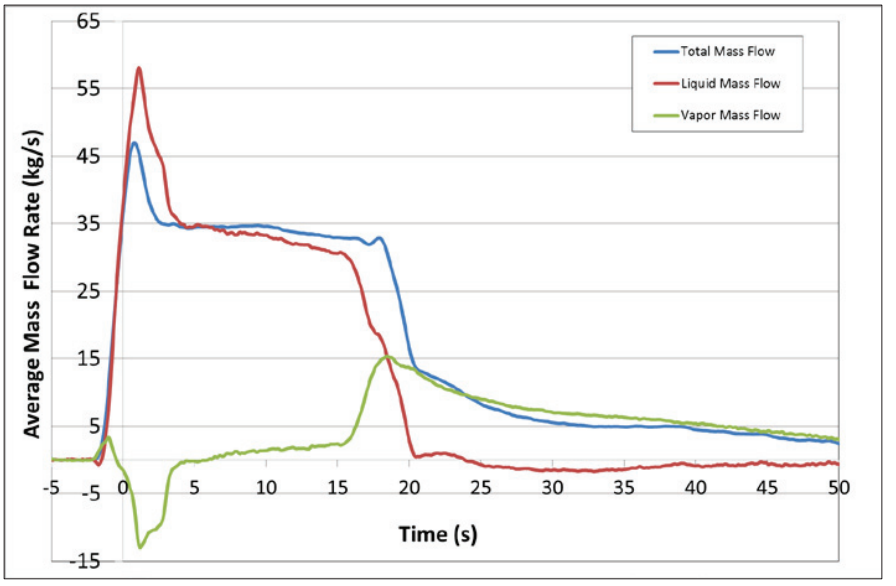

Figure 8 Mass flow rates for liquid and vapour out of the vessel. The blue line is the total mass flow, as is also depicted in Figure 3; the red line is the liquid mass flow rate and the green line is the vapour mass flow rate.

The blue line in Figure 8 is the total mass flow rate. The red and green lines are the liquid mass flow rate and the vapour mass flow rate, respectively. In the first transient it can be observed that the liquid mass flow is larger than the total mass flow, and that the vapour mass flow is negative. This is due to heavy boiling inside the vessel. This boiling reduces the amount of liquid more than the outflow by itself would do. That is the reason why the liquid flow rate is higher than the total mass flow rate.
During the stable stage the total mass flow rate and the liquid mass flow rate are nearly equal, indicating that the flow leaving the vessel is mainly liquid. After the second transient, this changes. The liquid mass flow rate decreases and the vapour outflow rate is nearly equal to the total outflow. This means that the outflow out of the vessel is either mainly liquid (stable stage; steady decrease) or mainly vapour (after 20 sec). The second transient is the transition between these two types of outflow.

4.5. Safety considerations: supercritical conditions vs saturated conditions

In this latter part, the concentrations measured and those obtained from the literature [5] are discussed, and plotted in the same graph. If the measurement points are not sufficient, a theoretical correlation can then be derived [10] to obtain the distribution of the CO_2 concentration inside the plume using the temperature and concentration measurements. Taking 5% v/v and 10% v/v CO_2 concentration as thresholds [14], it is possible to establish a curve giving the distance between the release point and the location where the iso-concentration is obtained. This distance envelope is plotted as function of the leakage flow rate in Figure 9. Power law behaviour can be observed on the graph for both values of concentration. In addition, no apparent differences are observed between initial saturated and supercritical conditions. From a safety point of view, the hazard distances do not seem to be affected by the initial supercritical or saturated conditions.

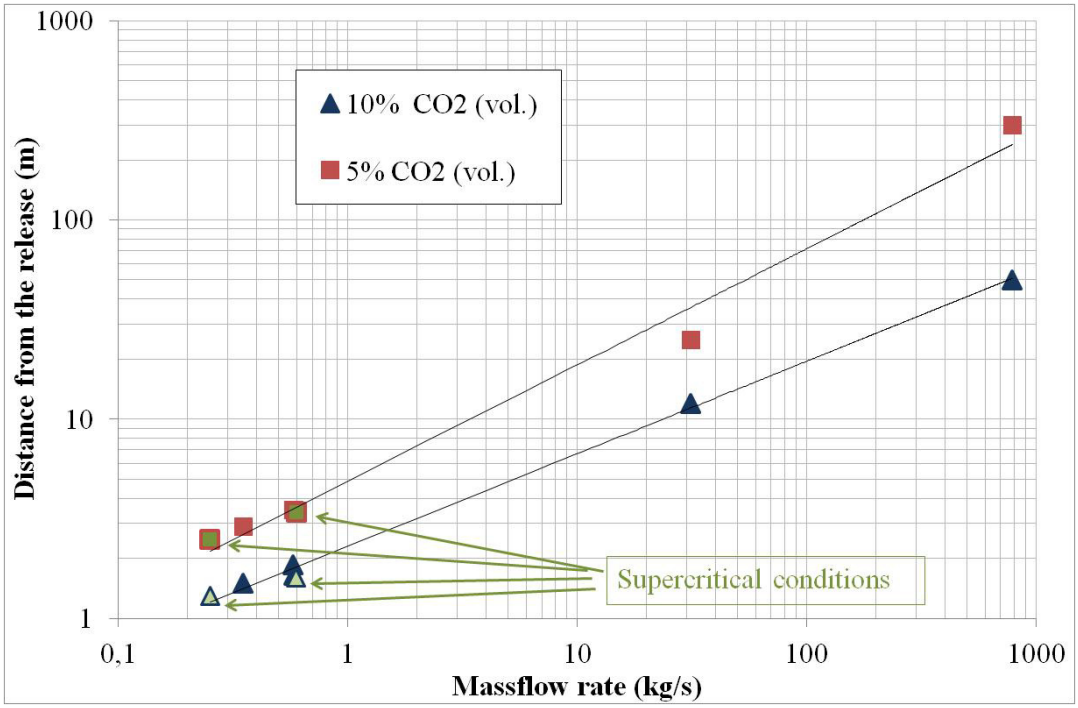

Figure 9: 5% and 10% CO_2 v/v isoconcentration distances, comparing supercritical vs saturated conditions [5,10]

5. Conclusions

INERIS and TNO have been involved in several CO_2 projects, dealing with the safety issues of CO_2 pipeline transport. In order to complete knowledge and expand the experimental database of CO_2 releases, tests have been run with INERIS test facilities to study the influence of the storage conditions (supercritical vs saturated), and the thermodynamical behaviour of the flow during a rapid blowdown of a vessel.
These trials allowed us to have a better understanding of the two-phase behaviour in the vessel and the flow - at several points along – inside the pipe, so that we can follow the release on a pH diagram. This will be helpful to develop and improve source term models.
The supercritical condition tests do not demonstrate any special behaviour in terms of cloud dispersion, when compared to 'classical' saturated conditions. The safety distances obtained have been plotted versus the mass-flow rate for several conditions, combining several experiments.

Acknowledgement
"This research has been carried out in the context of the CATO-2-program (www.co2-cato.org). CATO-2 is the Dutch national research program on CO2 Capture and Storage technology (CCS). The program is financially supported by the Dutch government (Ministry of Economic Affairs) and the CATO-2 consortium parties."

References

[1] Lilliestam J, Bielicki J.M., Patt A.G. Comparing carbon capture and storage (CCS) with concentrating solar power (CSP): Potentials, costs, risks, and barriers. Energy Policy 47, 2012.p.447–455
[2] Geske J., Berghout N., Van den Broek M. Cost-effective balance between CO_2vessel and pipeline transport. International Journal of Greenhouse Gas Control 36, 2015.p.175–188
[3] Sim S., Cole I.S, Choi Y.S., Birbilis N. A review of the protection strategies against internal corrosion for the safe transport of supercritical CO_2 via steel pipelines for CCS purposes. International Journal of Greenhouse Gas Control 29, 2014.p.185–199
[4] Woolley R.M., Fairweather M., Wareing C.J., Falle S., Mahgerefteh H., Martynov S., Brown S., Narasimhamurthy V., Storvik I., Sælend L., Skjold T., Economou I., Tsangaris D., Boulougouris G., Diamantonis N., Cusco L., Wardman M., Gant S., Wilday J., Zhang C.Y., Cheng S., Proust C., Hébrard J. and Jamois D. CO2PipeHaz: quantitative hazard assessment for next generation CO_2 pipelines. Energy Procedia 63, 2014.p.2510–2529
[5] Ahmad M., Bögemann-van Osch M., Buit L., Florisson O., Hulsbosch-Dam C., Spruijt M., Davolio F. Study of the thermohydraulics of CO_2 discharge from a high pressure reservoir. International Journal of Greenhouse Gas Control 37, 2015.p.340–353
[6] Woolley R.M., Fairweather M., Wareing C.J., Falle S.A.E.G., Proust C., Hébrard J., Jamois D. Experimental measurement and Reynolds-averaged Navier–Stokes modelling of the near-field structure of multi-phase CO_2 jet releases. Int. J. Greenhouse Gas Control 18, 2013.p.139–149
[7] Woolley R.M., Fairweather M., Wareing C.J., Proust C., Hebrard J., Jamois Narasimhamurthy, I.E. Storvik, T. Skjold, Falle S.A.E.G., S Brown S., Mahgerefteh H., Martynov S., Gant S., Tsangaris D.,,. Economou I.G, G.C. Boulougouris G, Diamantonise N.,An integrated, multi-scale modelling approach for the simulation of multiphase dispersion from accidental CO_2 pipeline releases in realistic terrain, 2014.p.221-238
[8] Kruse H. and Tekiela M. Calculating the consequences of a CO_2-pipeline rupture. Energy convers. Mgmt vol. 37, n°6-8, 1996.p. 1013-1018
[9] CO2QUEST: Techno-economic assessment of CO_2 quality effect on its storage and transport
[10] Jamois D., Proust C., Hébrard J., "Hardware and instrumentation to investigate massive releases of dense phase CO_2", The Canadian Journal of Chemical Engineering, vol. 93, issue 2, 2014.p.234-240
[11] NIST: http://webbook.nist.gov/
[12] H. K. Fauske, Determine Two-Phase Flows During Releases. *Chem. Eng. Progress*, 1999.p132-134
[13] S. Brown, S. Martynov, H. Mahgerefteh, C. Proust, A homogeneous relaxation flow model for the full bore rupture of dense phase CO_2 pipelines, 2013.p.349-356
[14] Note du 16/11/07 relatif à la concentration à prendre en compte pour l'O2, le CO2, le N2 et les gaz inertes. Ministère de l'écologie du développement durable et de l'énergie.